

An Application of Active Control to the Collector of a High-Speed Pantograph: Simulation and Laboratory Tests

A. Collina, A. Facchinetti, F. Fossati, F. Resta

Abstract— The current collection for the traction motor of trains is obtained by means of a sliding contact between the overhead line (OHL) and the collector strips mounted on the pantograph head. As the train speed increases, the variation of contact force exchanged between the pantograph and the OHL, dependent on their dynamic interaction, becomes greater. This condition causes excessive mechanical wear and contact wire uplift (for high values of contact forces), and leads to high percentage of loss of contact, arcing and electrically related wear if too low values of contact forces occur. The topic of actively controlled pantograph is gaining more interest as a tool to increase the performance of current collection. This paper describes authors research activities on this topic.

I. INTRODUCTION

The development of the European railway high speed network brings new problem related to the interoperability among the railways of different countries. On the other hand, the high investments necessary for the new high speed lines have raised the interest in the possibility of upgrading the existing line, in order to speed up the traffic also in these routes. The two main elements involved with the current collection are the pantograph and the catenary (OverHead Line, OHL). The pantograph, whose aim is to keep the contact with the OHL, enabling the power supply from the OHL to the electric motors of the train, is essentially a mechanical system, composed of an articulated frame, carrying a single or a double collector head, on which the collector strips for the electrical contact are mounted. The dynamic interaction between the pantograph and the OHL causes variations of the contact force around the mean value due to the static pre-load (usually given by an air bellow) and also caused by the mean aerodynamic uplift force due to the incident flow on the pantograph. The dynamic contact force variation, superposed to the mean contact force, can cause contact losses, arcing and sparking, with a deterioration of the quality of current collection and an increase of the electrical related wear, thus becoming a limiting factor for the maximum train speed. The increase of the static contact force is not an efficient way to solve the problem, because it increases mechanical abrasive wear and excessive uplift of

the contact wire can occur at suspension.

Therefore an optimization of both pantograph and catenary should be carried out in order to improve their performance. This approach can be followed for new design catenary, while for the speed-up of already existing line the active control of the pantograph could be an attractive way to solve the problem [11].

In order to reduce the effect of the above mentioned problems, the topic of actively controlled pantograph is gaining more interest as a tool to increase the performance of the current collection at high speed. Aim of this paper is to provide a review of the activities carried out by the authors on this topic.

II. GENERAL CONSIDERATION ON ACTIVELY CONTROLLED PANTOGRAPH AND LINE OF RESEARCH

When considering controlled pantographs [3] the actuators can be placed a) on the articulated frame[10], or b) in correspondence of the collector head suspension [1]. The first configuration has the advantage that there are no strict limitations to the size, power, mass and kind of the actuators (pneumatic, hydraulic or electric). Nevertheless, as pointed out in [1] and also shown in the following, its effectiveness is limited to the low frequency range (up to $1\div 2$ Hz), related to the span passing frequency, while at high speed (i.e. $V > 220$ km/h), the main contribution to the contact force variation come from the droppers' passing frequency ($10\div 20$ Hz). The second configuration is more effective for the control of the medium frequency range (up to 20Hz), but it imposes limitations to the size and mass of the actuators that have to be placed in correspondence of the collector head suspension. In spite of these difficulties, a solution for the second configuration has been looked for using a simple model of pantograph-OHL system. Subsequently, the selection of the actuators has been performed by means of a detailed complete model of the system. The investigation has been applied to pantograph ATR95 developed by Ansaldo Breda for the ETR500 train set. The activities related to the research have been developed through the following steps:

- preliminary assessment of the feasibility of the control configuration, by means of a simplified model of pantograph-catenary interaction, adopting a simple proportional control scheme, where the controlled variable is the contact force. Aim of the simplified model is to roughly define the control system configuration [7];
- refinement of the results from the previous step, by

Manuscript received March 14, 2005.

A. Collina, A. Facchinetti and F. Resta are with the Department of Mechanical Engineering, Politecnico di Milano, via La Masa, 34, 20158 Milan, Italy (e-mail: andrea.collina@polimi.it, alan.facchinetti@polimi.it, ferruccio.resta@polimi.it).

F. Fossati is with the Department of Industrial and Mechanical Engineering, University of Catania, viale Andrea Doria, 6, 95125 Catania, Italy (e-mail: fabio.fossati@polimi.it).

means of a complete model of the pantograph-catenary dynamic interaction, considering ideal actuators;

- selection of a suitable actuator, and evaluation of its installation on the real pantograph;
- modelling of the actuator dynamics and implementation of the controlled actuator in the complete model for the pantograph-catenary dynamic interaction [13];
- application of the active control to the extension of the travelling train speed, simulating an existing pantograph - catenary combination.
- set-up of a dedicated laboratory bench, where a single collector is controlled by a DC motor, for a preliminary validation of control strategies.

III. PRELIMINARY ANALYSIS WITH A SIMPLIFIED PANTOGRAPH-CATENARY MODEL

In order to assess the feasibility of the control system and of the actuating configuration, a simple model of the pantograph-catenary interaction has been adopted, based on a model already developed in [8] for diagnostic purposes. The OHL, consisting of three consecutive spans (figure 1), is modelled by means of a tensioned beam, whose characteristics are the sum of the characteristics of the contact wires and the messenger wires of the real catenary. The considered catenary (type C540 [6]) is composed of two messenger wires (with a cross section of 120mm² and a tension of 16000 N each) and two contact wires (with a cross section of 150mm² and a tension of 18750 N each). The transversal displacement $w(\xi, t)$ of the generic catenary point can be written in terms of vibration mode functions Φ_n and modal co-ordinates q_n :

$$w(\xi, t) = \underline{\Phi}(\xi)^T \underline{q}(t) \quad (1)$$

where $\underline{\Phi}$ is the vibration mode vector, containing the modal shapes of the tensioned beam with length $3L$, and \underline{q} is the modal co-ordinate vector (time depending only). A spring of suitable stiffness k_s is placed at each extremity of the central span. The pantograph model is based on a two degrees of freedom system. The mass m_h (representing the collector head) is supposed to be always in contact with the overhead line. Therefore the collector head vertical displacement, velocity and acceleration (figure 1) can be written as:

$$\begin{aligned} x_h &= \underline{\Phi}(Vt)^T \underline{q}(t); & \dot{x}_h &= V \underline{\Phi}'(Vt)^T \underline{q} + \underline{\Phi}(Vt)^T \dot{\underline{q}} \\ \ddot{x}_h &= V^2 \underline{\Phi}''(Vt)^T \underline{q} + 2V \underline{\Phi}'(Vt)^T \dot{\underline{q}} + \underline{\Phi}(Vt)^T \ddot{\underline{q}} \end{aligned} \quad (2)$$

where V is the train speed, and the prime ' denotes the spatial derivatives with respect to the abscissa ξ .

Following the Lagrangian approach, the equations of motion of the overall system (pantograph+OHL) are:

$$[M(t)]\ddot{\underline{x}} + [R(t)]\dot{\underline{x}} + [K(t)]\underline{x} = \underline{Q} \quad (3)$$

where \underline{x} is the vector of the independent variables, i.e. the base frame displacement and modal co-ordinates of the overhead line:

$$\underline{x} = \{x_f \quad q_1 \quad q_2 \quad \dots \quad q_n\}^T \quad (4)$$

The vector \underline{Q} represents the lagrangian component of the active force, which are the preload applied to the articulated frame of the pantograph, and the force due to the active control.

The system matrices in (3) represent the catenary mass damping and stiffness matrices which are time depending due to the pantograph position along the contact wire $\xi = Vt$.

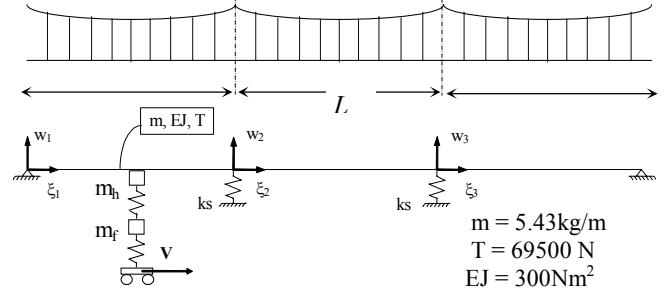


Fig. 1: simplified model for Pantograph-catenary interaction

The equations of motion are numerically integrated in the time domain, with a special procedure that enables the pantograph to run always in the central span, simulating the passage under a number of spans as required.

The control system is based on a feedback of the contact force between the collector head and the OHL. The control force is evaluated by a proportional – integral control of the difference between the reference value (mean value) and the measured one:

$$F_c = k_p (F_{ref} - F_{meas}) + \int k_i (F_{ref} - F_{meas}) dt \quad (5)$$

At the present stage, the research is focused on the feasibility of the active control, i.e. considering the performance that can be achieved adopting an already available actuator. The analysis has been performed applying the force directly to the collector head suspension or to the pantograph articulated frame.

The first solution has been preferred in terms of dynamic response of the control system. Figure 2 reports the contact force between pantograph and OHL at 250 km/h numerically obtained without control. The successive figure 3, shows the same quantity adopting active control with the actuator placed on the articulated frame. With this configuration there's a decrease in the first harmonic component of the contact force spectrum, while the higher harmonics are not decreased. Figure 4 is relevant to the active control placed on the collector head.

Comparing the two solutions, it can be seen that the effectiveness of the active control positioned on the collector head is higher. This is due to the fact that only the lower frequencies are involved with the articulated frame dynamics: therefore higher frequencies of the contact force can not be easily controlled with a simple PI regulator acting on the articulated frame. Moreover, keeping in mind that the simplified model does not take into account for the droppers, it can be concluded that the most efficient location of the control is on the collector head.

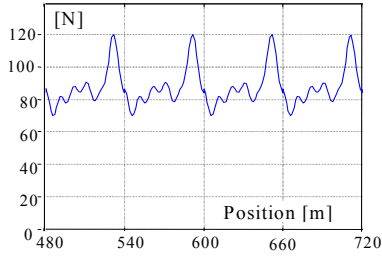


Fig. 2: Contact force obtained from the simplified model: without control

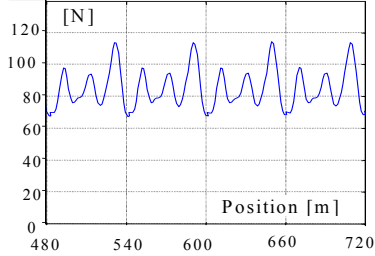


Fig. 3: Contact force obtained from the simplified model: active control on the articulated frame

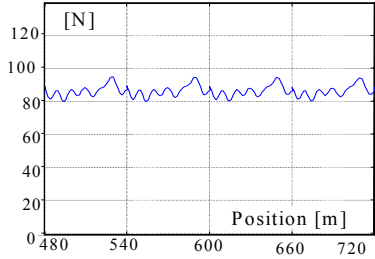


Fig. 4: Contact force obtained from the simplified model: active control on the collector head

IV. VERIFICATION WITH A COMPLETE PANTOGRAPH-CATENARY MODEL

The second step was the application of the previously defined control between the collector head and the articulated frame in the complete pantograph–catenary model, considering ideal actuators. A detailed description of the simulation model is already described in [7]. Only the main features will be reported here.

A. Mathematical model of the full catenary

In the full OHL schematization Bernoulli-Euler 2-node tensioned beam element are adopted for contact wire, messenger wire, and auxiliary wires (if present). Boundary conditions are set up by means of springs, as well as for supports at each span, while registration arm is reproduced with a lumped mass. The number of considered span is 15. The equations of motion are written through a lagrangian approach, around the static equilibrium position:

$$[M_c]\ddot{\underline{x}}_c + [R_c]\dot{\underline{x}}_c + [K_c]\underline{x}_c = \underline{F}_c(\underline{x}_c) + \underline{F}_{cp}(\underline{x}_c, \dot{\underline{x}}_c, \underline{x}_p, \dot{\underline{x}}_p, t) \quad (6)$$

where \underline{x}_c collects the d.o.f of the finite element schematization of the catenary, $[M_c]$, $[R_c]$ and $[K_c]$ are respectively mass, damping and stiffness matrices, being $[R_c] = \alpha[M_c] + \beta[K_c]$. The term \underline{F}_{cp} and \underline{F}_c are respectively the generalised force vectors related to the contact force exchanged between the pantograph and the contact wire and to the non-linear droppers' behavior. The vertical motion of

the contact point travelling along the longitudinal direction with a speed V , is expressed through the shape function of the k -th finite element, where the contact point is located at time t .

B. Mathematical model of the pantograph and its interaction with the OHL

For the pantograph, a lumped parameter model is adopted. The d.o.f. of the model of the pantograph (see figure 5) are: the rotation of the front (φ_1) and rear (φ_2) collector heads, the rotation α and the vertical motion z_q of the pan-head. The equations of motion of the pantograph are the following:

$$[M_p]\ddot{\underline{x}}_p + [R_p]\dot{\underline{x}}_p + [K_p]\underline{x}_p = \underline{F}_{pc}(\underline{x}_c, \dot{\underline{x}}_c, \underline{x}_p, \dot{\underline{x}}_p, t) \quad (7)$$

where \underline{x}_p is the pantograph displacements vector, M_p , R_p and K_p are the mass damping and stiffness pantograph matrices, \underline{F}_{pc} represents the vector of the generalised forces including static pre-load and contact forces (depending both on overhead line dynamics and pantograph dynamics).

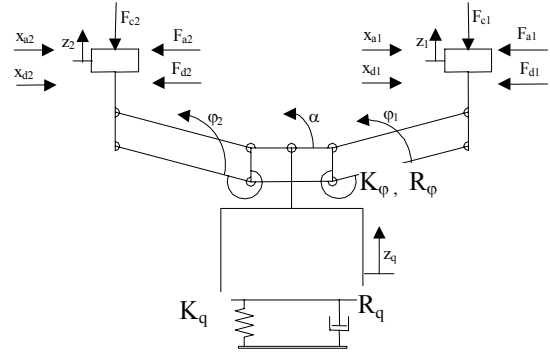


Fig. 5: Model of the pantograph for the complete model of pantograph-OHL interaction

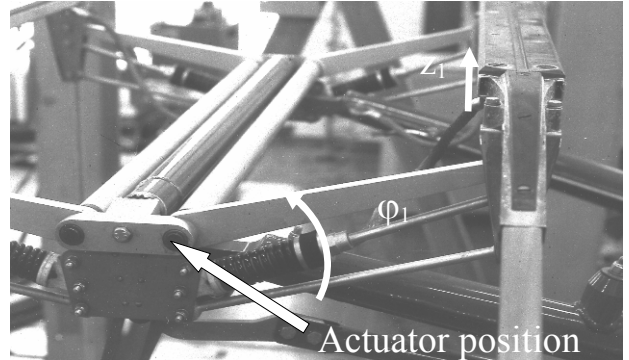


Fig. 6: Location of the actuators on the pantograph head

C. Model of the actuator

The active control of the pantograph is realised by controlling the rotations φ_1 e φ_2 of both collectors. This is obtained by means of two electric motors applied inside the joint between pan-head and each collector head arm (fig. 6). The actuator consists in a electromechanical system including a DC motor and a gearbox. DC servomotors with relatively small power ratings characterised by extremely small time constants and the high torque-to-inertia ratio have been chosen. The armature –controlled DC motor is driven by an electronic controller operating in torque control mode.

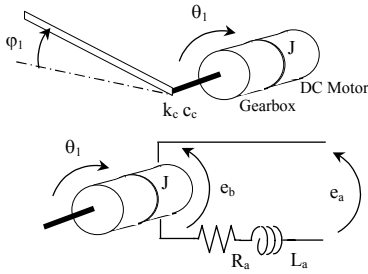


Fig. 7 – Mechanical and electrical model of the actuator

Considering the armature controlled DC servomotor shown in figure 7, where the field is held constant, the torque T developed by the motor is proportional to the armature current i_a :

$$J\ddot{\theta} + c\dot{\theta} = T - T_r = ki_a - T_r \quad (8)$$

T_r represents the torque acting on the actuator rotor due to the moment applied to each individual collector head. J is the rotary inertia of the motor shaft and c is an equivalent viscous damping constant. The speed of an armature-controlled DC servomotor is controlled by the armature voltage e_a , that is the input of the power controller. The differential equation for the armature circuit is:

$$L_a \frac{di_a}{dt} + R_a i_a + e_b = e_a \quad e_b = k_b \dot{\theta} \quad (9)$$

being L_a and R_a the inductance and resistance of the circuit, e_b the back e.m.f and k_b is the back e.m.f. constant.

The e_a voltage is evaluated by the control system as a function of the reference and measured contact forces:

$$e_a = k_p (F_{ref} - F_{meas}) + \int k_i (F_{ref} - F_{meas}) dt \quad (10)$$

The electric motor (see figure 7) is placed on the pantograph, in order to apply the desired torque to the bars of the suspension of the collector head, through a gearbox reduction τ . The torque T_r can be evaluated by means of the following expression:

$$T_r = k_c \tau (\tau \dot{\theta} - \dot{\varphi}) + c_c \tau (\tau \dot{\theta} - \dot{\varphi}) \quad (11)$$

where the terms k_c and c_c account for the stiffness and damping of the mechanical coupling between the output shaft of the gearbox and the bar of the suspension of the collector. The state vector of both actuators is:

$$x_a = \{\dot{\theta}_1 \quad \dot{\varphi}_1 \quad i_{a1} \quad \dot{\theta}_2 \quad \dot{\varphi}_2 \quad i_{a2}\}^T \quad (12)$$

where the index 1,2 refers to the front and rear actuator respectively. The corresponding state equations can be obtained, from (8) to (12):

$$[A_a] \dot{x}_a + [B_a] x_a = E_a(\varphi_i, \dot{\varphi}_i, F_{ref}, F_{meas}) = E_a(x_p, \dot{x}_p, F_{ref}, F_{meas}) \quad (13)$$

Mass [kg]	0.44
J [kg m ²]	84.7E-7
c [Nm/s]	3.7E-6
L_a [H]	2.E-3
R_a [ohm]	1.9
k [Nm/A]	4.2E-2
k_b [Vs/rad]	42.4E-3
τ	1/100

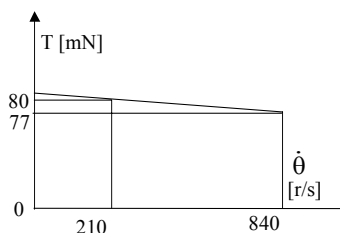


Table I – actuator main data and its mechanical characteristic

D. The complete pantograph-catenary model

Overhead line, pantograph and actuators equations of motion are solved by means of a numerical integration method and represent the dynamic behaviour of the whole system. Combining eqs.(6), (7) and (13), the following set of equations of motion are obtained:

$$\begin{cases} [M_c] \ddot{x}_c + [R_c] \dot{x}_c + [K_c] x_c = F_{ac}(x_c) + F_{cp}(\dot{x}_p, x_p, \dot{x}_c, x_c, t) \\ [M_p] \ddot{x}_p + [R_p] \dot{x}_p + [K_p] x_p = F_{pc}(x_c, \dot{x}_c, \dot{x}_p, x_p, x_a, t) \\ [A_a] \dot{x}_a + [B_a] x_a = E_a(x_p, \dot{x}_p, F_{ref}, F_{meas}) \end{cases} \quad (14)$$

The forcing terms F_{cp} and F_{pc} act as coupling terms between the two sets of equations and therefore include in the model the effects of pantograph-OHL interaction.

V. SIMULATION RESULTS

First the contact condition with the standard configuration is shown for the leading (figure 8) and the trailing collector (figure 9) of the pantograph. The phenomenon of the unequal distribution of mean contact force on the two collectors is put in evidence, as also found experimentally [6]. This phenomenon is due to the effect of drag aerodynamic forces and friction forces acting on both collectors. Looking at figure 5, it is quite evident that the longitudinally applied forces cause a variation of the vertical contact forces. In this condition, the efficiency of the second collector is very poor, with a high contact loss percentage (12%).

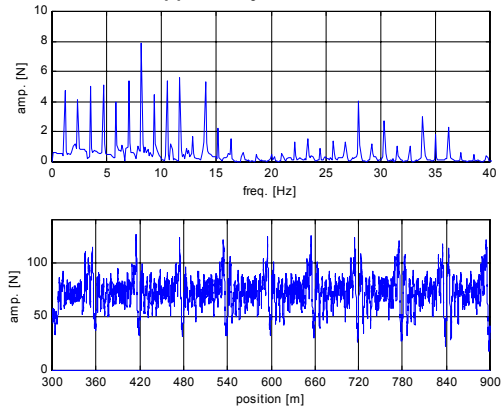


Fig. 8: Contact force on the front collector: without control

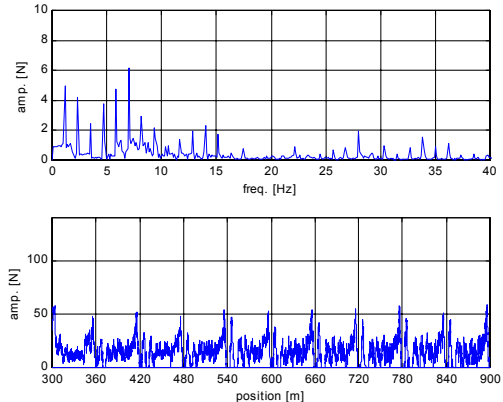


Fig. 9: Contact force on the rear collector: without control

The mean contact force (see Tab.II) is higher on the front collector (73N), and much lower on the rear one (15N). The control action is applied on each collector head, first considering ideal actuators. The results obtained from these simulations allowed the proper selection of the power required by the actuator. The following results refer to the complete model, including the model of the actuators, as described in the previous paragraph.

The effect of the active control is shown in the figures 10-11: in this case the reference value of the force for each collector is set at 45N. The improvement due to the active control is evident: as it can be seen the contact force of the rear collector goes to zero only sporadically, while on the uncontrolled case the loss of contact is very frequent. The active control partially succeeds also in equalizing the mean contact force on the two collectors.

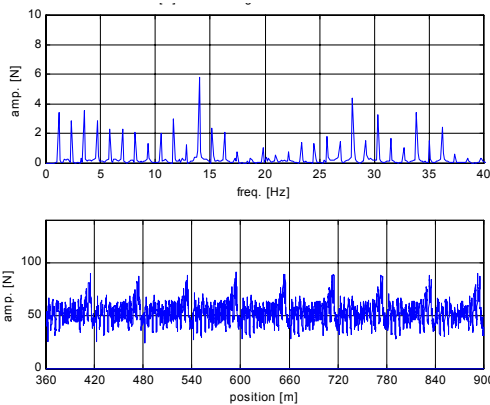


Fig. 10: Contact force on the front collector: with control

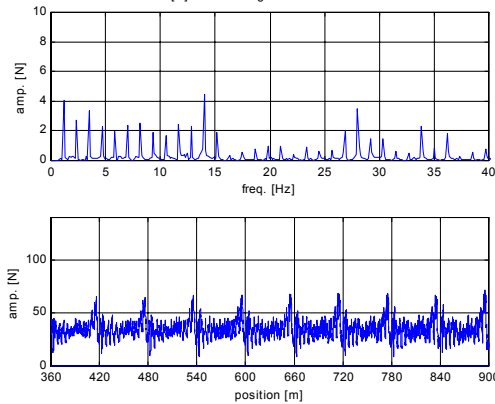


Fig. 11: Contact force on the rear collector: with control

	I collector		II collector	
	F_m [N]	σ [N]	F_m [N]	σ [N]
No control	73	15.2	15	11
Control	52.5	10.4	34.5	8.9

Table II: Summary results at 250km/h

Tab. III reports the peak values and the R.M.S. values of the electrical power and of the torque. On the basis of these results the compatibility with motor characteristic can be verified: it can be observed, that the R.M.S. value of the torque is within the permissible range of operation of the motor. It has also been verified that the maximum rotating speed (about 100 rad/s) is within the motor operating range.

	Torque (RMS)	Torque (peak)	Power (peak)	Power (mean)
Front	70.7mNm	250mNm	120W	10.84W
Rear	64.5mNm	160mNm	60W	9.1W

Table III: actuators performance at 250km/h

Since one of the aim of the actively controlled pantograph is to increase the train speed with respect to the design speed of the line, without modifications of the OHL, the extension of the maximum allowable train speed from 250 km/h to 300 km/h has been checked. In figures 12–13 the performance index of the contact force, defined as $F_{mean-3\sigma}$, is reported for both collectors, as a function of the train speed.

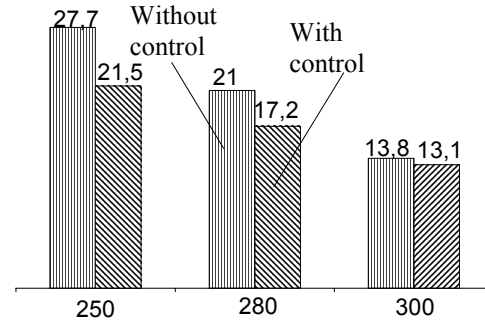


Fig. 12: Performance index [N] of the front collector vs train speed [km/h]

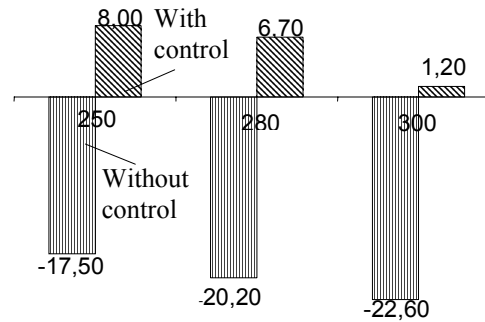


Fig. 13: Performance index [N] of the rear collector vs train speed [km/h]

As can be seen the performance index with the active control is always positive and the behaviour of the two collectors are balanced allowing a more efficient current collection. This is due to two different reasons: the mean contact force of both collectors approaches the reference value, i.e. it decreases for the front collector (where it is too high), and increases for the rear one (where it is too low), reducing the force unbalance related to the pantograph architecture. Moreover, the standard deviation of both collectors is decreased by the action of the active control. Both these effects increase the performance index, therefore improving the current collection quality.

VI. PRELIMINARY LABORATORY BENCH

A preliminary laboratory bench has been setup where the active control of the pantograph is realised by controlling a single collector. This is obtained by means of an electric motor applied inside the joint between pan-head and the collector head arm (fig. 14), according to the previously

described numerical simulations. The armature –controlled DC motor is driven by an electronic controller operating in force control mode.

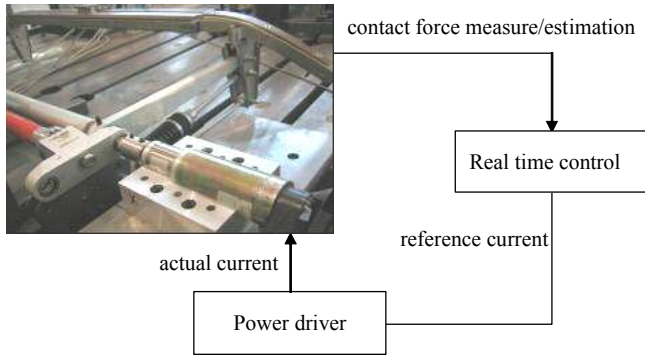


Fig. 14: Pantograph active control

The collector is coupled with the edge of a beam which presents a moving constraint in order to achieve a variable stiffness (Fig. 15). The moving constraint is realized by means of a linear actuator. The dimension of the beam and the amplitude of the constraint harmonic motion have been chosen in order to reproduce the catenary stiffness variation corresponding to span passing.

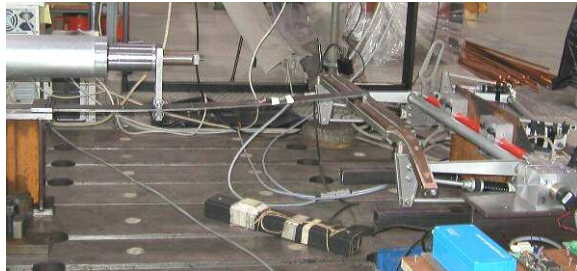
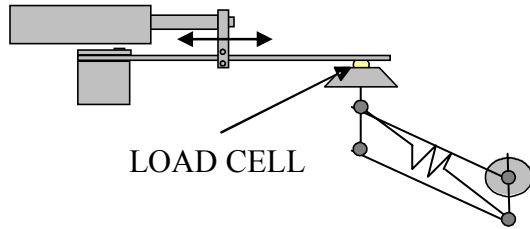


Fig. 15: Preliminary laboratory test bench

On the laboratory test bench, three different type of control (R, fig. 16) have been analyzed: proportional, with 2 poles and 2 zeros and with 4 poles and 4 zeros.



Fig. 16

The first considered control is a simple proportional regulator on contact force error. The value of the proportional gain k_p is chosen in order to keep a minimum acceptable system stability: the proportional control does not modify significantly the position of the poles of the system and leads to a decrease of the damping associated with the first natural frequency (approximately 4 Hz), which get

closer to an instability condition.

Figure 17 shows the presence of frequencies multiples of the span passing frequency (approximately 1 Hz), due to the non-linearities of the coupled systems. The first harmonic component related to span passing is reduced of the 45% while the components with frequencies between 3 and 6 Hz are amplified by the proportional control, as a consequence of the reduced damping.

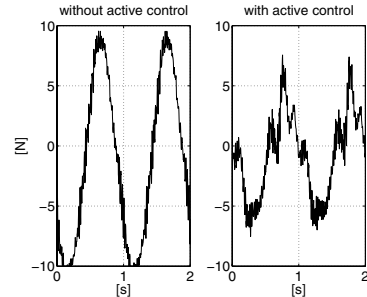


Figure 16: Contact force variation (proportional controller)

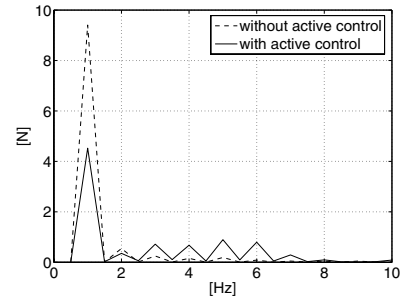


Fig. 17: Contact force spectrum (proportional controller)

With the purpose to improve the performances of the controlled system, a 2 poles and 2 zeros controller has been checked.

The zeros of the controller are placed in order to increase the damping of the first system natural frequency and to avoid instability approaching when controller gain increases. Problems related to negative damping and consequent instability are therefore transferred to the second natural frequency of the system. The 2 poles of the controller, which are necessary for the controller feasibility, are placed in order to filter the higher frequencies without introducing significant phase shifts in the frequency range of interest. Moreover the chosen position of controller poles permits to limit the control variable, armature current i_{rif} (fig. 16), and to avoid the saturation of actuator power.

The gain of the controller, being all the other parameters fixed in order to obtain the described zeros and poles position, affects system stability as reported in figure 18, which shows the simulated contact force spectra for different values of the controller gain.

For this reason, the controller gain must be limited in order to avoid system instability related to the second natural frequency of the system (approximately 11 Hz). As a consequence, the maximum achievable improvement is a reduction of the first harmonic component related to span passing of the 45%, as for the proportional control, without

affecting the frequencies in the range between 3 and 6 Hz.

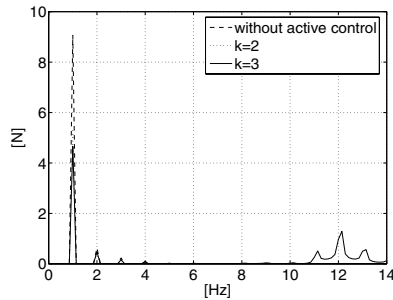


Fig. 18: Simulated contact force spectrum (2 poles and 2 zeros controller)

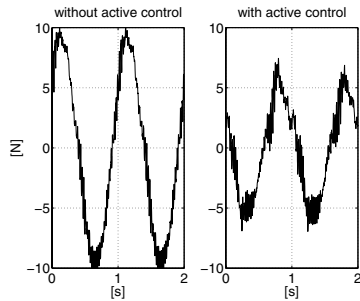


Fig. 19: Contact force variation (2 poles and 2 zeros controller)

In order to obtain further improvement 2 other zeros were added to enhance the dynamic behaviour in the frequency range around 11 Hz, together with other 2 poles necessary for control feasibility.

The poles position was chosen corresponding to the distribution of a Butterworth 4th order filter, with a cut-off frequency of 20 Hz.

With this solution, the gain of the controller could be increased up to achieve a reduction of the first harmonic component related to span passing of the 67%, without affecting all the other frequencies of interest (fig. 20-21).

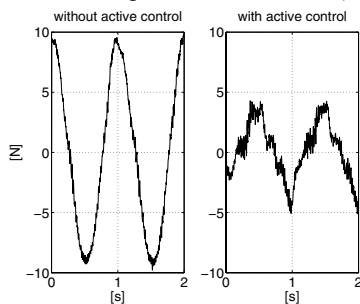


Fig. 20: Contact force variation (4 poles and 4 zeros controller)

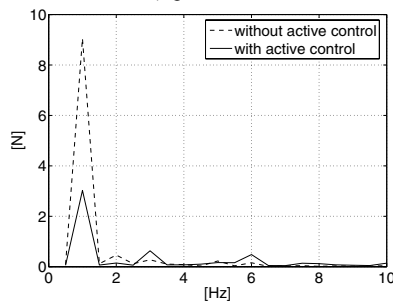


Fig. 21: Contact force spectrum (4 poles and 4 zeros controller)

The performances of the controlled system could be improved even more, adopting a notched filter tuned to the

span crossing frequency. However this solution was not considered since the span crossing frequency is strictly related to the train speed and to the type of OHL, parameters which may vary significantly along the track.

VII. THE HARDWARE IN THE LOOP TEST-RIG

The natural prosecution of the preliminary described set-up is to analyse the dynamic behaviour of a complete pantograph and catenary system. For this purpose a laboratory test rig is being set-up in order to take into account both the pantograph dynamics due to the catenary motion and the catenary response due to the contact force.

The idea [14] consists in installing a pantograph in the laboratory and coupling the collectors with a displacement controlled hydraulic cylinder. The control system imposes to the hydraulic cylinder a motion law derived by a numerical model of the catenary excited by the contact forces, actually measured in the test-rig.

In this way, the pantograph is moved by the actuator which imposes the displacements of the collectors: the contact force between the pantograph and the hydraulic actuator is measured and feedback in the catenary model.

A Hardware In the Loop (HIL) device has been in this way realised: the real pantograph dynamics is coupled to a hydraulic cylinder controlled by a PC (Fig. 22). A simplified numerical model of the catenary, forced by passing of the directly measured contact force, allows us to evaluate the time history of the displacements of the point of the line in contact with the collector. In real time, this time history is imposed as references to the control system of the actuator.

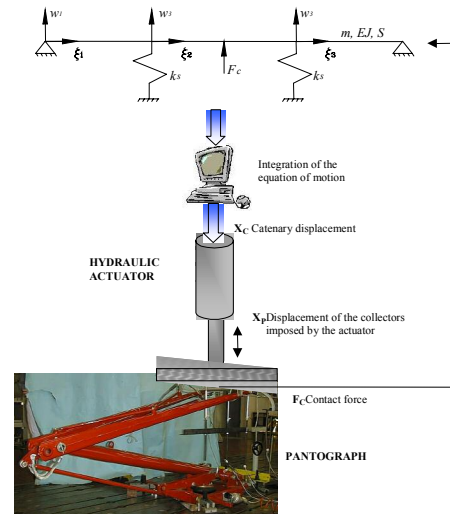


Fig. 22: The Hardware in The loop test rig scheme

The feasibility of the proposed approach was previously checked simulating the complete experimental set-up by means of a numerical model, realised with Simulink.

After the numerical validation of the test rig design [4], a pantograph and a hydraulic actuator have been installed in the laboratory and the catenary model has been implemented into a acquisition and control board (Dspace 1102 based on

DSP Texas TMS320C31), which is programmable using an high level interface in SIMULINK/MATLAB[®] environment. The board interact with the bench through an analog input, represented by the measure of the actual contact force between the hydraulic actuator and the pantograph, and an analog output, consisting in the reference position required to the actuator. Figure 23 shows a picture of the realised test-rig.



Fig. 23: The hardware in the loop test-rig

VIII. CONTACT FORCE MEASUREMENTS/ESTIMATION

In this work the contact force plays the role of the control variable: it is worth mentioning that the problem of the measurement of the contact force has not been considered yet. It is known that contact force measurement is a challenging task, especially due to the adverse environmental condition (e.m. disturbances, high vibration levels), and to the limitation of the frequency range. The maximum frequency that can be obtained is about 15-20 Hz [5], in order to suppress the effect of the inertial terms related to the deformable modes of the collector.

Filtering of contact force measures causes a time delay, which decrease the performance of the controller. An alternative way to get the contact force is to estimate it by means of the extended Kalman filter, as proposed in [3,9], on the basis of the measurement of the displacements and velocities of the pantograph elements (articulated frame and collectors).

IX. CONCLUSIONS

An active control for an existing pantograph has been proposed, based on an existing commercial actuator, and its feasibility and effectiveness have been investigated by means of numerical simulation. At this purpose, the dynamics of the actuator (a permanent DC motor) has been included in a complete pantograph-catenary interaction model.

Some simplifying assumptions have been made concerning the measurements of the contact force: this aspect will be considered in the prosecution of the work, both including the real performance of the measurement system, and substituting the measurements with the estimation of the force, based on the EKF.

The application of the active control appears promising, even if the previous experimental applications have encountered many practical problems, and have not been so satisfactory up to now [2,10]. Due to this reason, the real implementation of the proposed electrical actuator will be prior performed on a laboratory test rig, where it will be possible to set-up the control. The adopted control strategy is based on a simply PI regulator, better performance could be obtained with more sophisticated approaches [12].

Anyway the indications obtained from the simulation with the complete pantograph catenary model show the capability of the active control to increase the train speed on existing catenaries, thus avoiding expensive catenary upgrading, and also enabling to decrease the mean contact force, thus decreasing the mean mechanical abrasive wear.

Future developments involves the installation of the complete pantograph with the active controller on the HIL simulator, and the introduction of droppers contribution in the numerical model adopted for driving the hydraulic actuator, in order to extend the range of reproducible frequency.

REFERENCES

- [1] K.A. Althammer, W. Baldauf, "Considerations on high performance pantographs", WCRR '99, Tokio, October 1999
- [2] K.A. Althammer, W. Baldauf, "Simulation of actively controlled pantographs in overhead line systems". WCRR '97, Florence, 16-19 Nov. 1997
- [3] D. Carillo, A. Collina, A. Facchinetti, F. Fossati, M. Papi, F. Resta, "Application of EKF to the estimation of contact forces in pantograph-catenary system", WCRR 2003, Edinburgh, UK, 2003
- [4] A. Collina, A. Facchinetti, F. Fossati, F. Resta, "Hardware in the loop test-rig for identification and control application on high speed pantographs", Shock and Vibration, Vol. 11, Nos. 3-4 (2004), pp.445-446, IOS Press
- [5] P. Delfosse, B. Sauvestre, "Mesure d'effort de contact entre pantograph et caténaire", RGCF, AVRIL 1983, 102 Annè, pp.203-212
- [6] G. Diana, M. Bocciolone, A. Collina, M. Papi, A.G. Violi, "Optimization of a new d.c. catenary by means of measurements and simulation of pantograph-catenary interaction", WCRR '99, Tokio, October 1999
- [7] G. Diana, S. Bruni, F. Fossati, F. Resta, A. Collina, "High speed railways: pantograph and overhead line modelling and simulation", Computer in Railways VI, WIT press 1998, pp.847-856
- [8] G. Diana, F. Fossati, F. Resta, A. Collina, "Active Control of high speed train pantograph", Illrd Int. Conf. On Motion on and Vibration Control, Chiba, 1-6 Sept. , 1996, Japan
- [9] G. Diana, F. Fossati, F. Resta, "High Speed Railway: Pantographs Active Control and Overhead Lines Diagnostics and Solutions", Veichle System Dynamics, Vol 30 (1988)
- [10] M. Papi, M. Rinci, A. Rindi, & P. Toni, "Preliminary field testing of a servoactuated pantograph", Computer in Railways VI, WIT press 1998, pp.837-846
- [11] G. Poetsch and oth., "Pantograph/Catenary Dynamics and Control", Veichle System Dynamics, Vol. 28(2/3), pp 159-195, 1997
- [12] D. N. O'Connor, S. D. Eppinger, W.P. Seering, D. N. Wormley, "Active Control of a High-Speed Pantograph", ASME Jour. Of Dynamic Systems, Meas. and Control, Vol. 119, N.1, March 1997
- [13] F. Resta, A. Collina, F. Fossati, "Actively controlled pantograph: an application", AIM '01, Como, Italy, July 2001
- [14] W. Zhang, G. Mei, X. Wu, Z. Shen, "Hybrid Simulation of Dynamics for the Pantograph-Catenary", Vehicle System Dynamics, Vol.38, N.6, pp. 393-414, 2002, Swets & Zeitlinger